Biosensors and Bioelectronics: X 15 (2023) 100392

Contents lists available at ScienceDirect

Biosensors and Bioelectronics: X

journal homepage: www.journals.elsevier.com/biosensors-and-bioelectronics-x

# μDACS platform: A hybrid microfluidic platform using magnetic levitation technique and integrating magnetic, gravitational, and drag forces for density-based rare cancer cell sorting

Seren Kecili [a,1], Esra Yilmaz [a,1], Ozge Solmaz Ozcelik [a], Muge Anil-Inevi [a], Zehra Elif Gunyuz [b], Ozden Yalcin-Ozuysal [b], Engin Ozcivici [a], H. Cumhur Tekin [a,c,*]

[a] Faculty of Engineering, Department of Bioengineering, Izmir Institute of Technology, Izmir, 35430, Turkey
[b] Faculty of Science, Department of Molecular Biology and Genetics, Izmir Institute of Technology, Izmir, 35430, Turkey
[c] METU MEMS Center, Ankara, 06520, Turkey

ARTICLE INFO

*Keywords:*
Hybrid cell sorting
Magnetic levitation
Circulating tumor cells
White blood cells
Label-free
Density
Biophysical biomarkers

ABSTRACT

Circulating tumor cells (CTCs) are crucial indicators of cancer metastasis. However, their rarity in the bloodstream and the heterogeneity of their surface biomarkers present challenges for their isolation. Here, we developed a hybrid microfluidic platform (microfluidic-based density-associated cell sorting (μDACS) platform) that utilizes density as a biophysical marker to sort cancer cells from the population of white blood cells (WBCs). The platform utilizes the magnetic levitation technique on a microfluidic chip to sort cells based on their specific density ranges, operating under a continuous flow condition. By harnessing magnetic, gravitational, and drag forces, the platform efficiently separates cells. This approach involves a microfluidic chip equipped with a microseparator, which directs cells into top and bottom outlets depending on their levitation heights, which are inversely proportional to their densities. Hence, low-density cancer cells are collected from the top outlet, while high-density WBCs are collected from the bottom outlet. We optimized the sorting efficiency by varying the flow rates, and concentrations of the sorting medium's paramagnetic properties using standard densities of polymeric microspheres. To demonstrate the platform's applicability, we performed hybrid microfluidic sorting on MDA-MB-231 human breast cancer cells and U-937 human monocytes. The results showed efficient sorting of rare cancer cells (≥100 cells/mL) from serum samples, achieving a sorting efficiency of ~70% at a fast-processing speed of 1 mL $h^{-1}$. This label-free approach holds promise for rapid and cost-effective CTC sorting, facilitating in-vitro diagnosis and prognosis of cancer.

## 1. Introduction

Rare cells, defined as those with a concentration of fewer than 1000 cells $mL^{-1}$ in a blood sample are important for the diagnosis and prognosis of many diseases, including cancer (Dharmasiri et al., 2010; Chen et al., 2014). These cells consists of circulating tumor cells (CTCs), circulating fetal cells (CFCs), hematopoietic stem cells (HSCs), and endothelial cells (Hyun et al., 2013; Shields Iv et al., 2015). CTCs are tumor cells in the bloodstream which spread from the primer tumor or metastatic site (Kim and Jung, 2010). In the peripheral blood of patients with metastatic cancers, CTCs can be found as low as 1 per $10^6$ white blood cells (WBCs) (Nagrath et al., 2007). In addition to their usage for cancer diagnosis, CTCs can also be used to understand the genetic and immunophenotypic differences that occur with tumor progression (Allard et al., 2004; Yap et al., 2014). Therefore, these cells have considerable potential for the development of targeted therapy and personalized medicine tools (Hyun et al., 2013). There are different methods for the detection, isolation, and characterization of CTCs (Kim and Jung, 2010; Allard et al., 2004). However, the utilization of CTCs in clinical practice is limited due to their low concentration and fragility, as well as low sorting efficiency of available technologies (Kim and Jung, 2010; Allard et al., 2004).

Antibody binding-based methods are generally used to separate rare cells from a heterogeneous cell population. These methods encompass

* Corresponding author. Faculty of Engineering, Department of Bioengineering, Izmir Institute of Technology, Izmir, 35430, Turkey.
*E-mail address:* cumhurtekin@iyte.edu.tr (H.C. Tekin).
[1] Both authors contributed equally.

https://doi.org/10.1016/j.biosx.2023.100392
Received 23 January 2023; Received in revised form 19 July 2023; Accepted 18 August 2023
Available online 26 August 2023

fluorescence-activated cell sorting (FACS) and magnetic-activated cell sorting (MACS) (Tomlinson et al., 2013). However, FACS and MACS have operational limitations, including high-cost implications, the requirement of a specialist and reduced cell viability during the sorting presence, and dependence on cell surface biomarkers (Gossett et al., 2010; Gascoyne et al., 2009; Lozar et al., 2020). Moreover, with these technologies, the isolation of different cancer types or subtypes with heterogeneous biomarker expression is limited and it may lead to low-sorting efficiencies. For example, antibodies against EpCAM (i.e., epithelial cell adhesion molecule) are commonly used for CTC isolation in many cancers such as colon, prostate, lung, and breast (Yousuff et al., 2016). However, different cancer subtypes demonstrate diversity in EpCAM expression (Königsberg et al., 2011), meaning that all CTCs cannot be efficiently isolated with these antibodies (Sieuwerts et al., 2009).

Label-free methods can also be used to sort cells according to their intrinsic physical properties, such as size, shape, density, adhesion strength, stiffness, deformability, and hydrodynamic, electrical, and optical properties (Gossett et al., 2010; Eifler et al., 2011). For instance, size-based separation was used in different microfluidic devices including filtration (Bussonnière et al., 2014), deterministic lateral displacement (Renier et al., 2017), inertial (Aghilinejad et al., 2019), centrifugal (Zhu et al., 2021), and acoustic force-based (Lee et al., 2014), and dielectrophoresis-field flow fraction (DEP-FFF) (Waheed et al., 2021) mechanisms. Using acoustic radiation force and laminar drag force, MCF-7 breast cancer cells were separated from nonmalignant leukocytes with 84% purity (Ding et al., 2014). DEP-FFF method was also used for sorting of HT-29 cancer cells from WBCs using both size and electrical properties (Shamloo et al., 2020). However, size-based methods have some drawbacks; CTCs may have a similar size range to white blood cells (Bankó et al., 2019). Density-based methods, allow the separation of cells based on their small density differences (i.e., red blood cell having densities of $>1.1$ g mL$^{-1}$, white blood cell having densities of $>1.08$ g mL$^{-1}$ and CTC having densities of $<1.08$ g mL$^{-1}$) (Norouzi et al., 2017; Morgan et al., 2007; Fehm et al., 2018). AccuCyte® (RareCyte) is a density-based separation system (Cho et al., 2018), it was combined with CyteFinder, which is an automated image analysis system, for the isolation and characterization of CTCs. For this purpose, firstly, the buffy coat was separated from blood using AccuCyte®, and single-cell imaging was made on a microscope slide with CyteFinder to reveal CTCs with cytoplasmic cytokeratin and EpCAM staining (Campton et al., 2015). However, the density-based separation system is limited by the requirement of multiple equipment and steps in the separation process, as well as the need for immunofluorescence staining of cells for image analysis (Yaman et al., 2018).

Paramagnetic salt solutions and ferrofluids have been widely used to levitate objects in the presence of magnetic and gravitational forces. This method is generally called magnetic levitation, or concisely "MagLev" (Yaman et al., 2018; Zhao et al., 2016). In recent years, magnetic levitation has been established as a novel label-free technology to measure densities at the single-cell level and manipulate cells/microparticles via negative magnetophoresis based on their unique densities and magnetic susceptibilities (Yaman et al., 2018; Zhao et al., 2016; Anil-Inevi et al., 2018; Durmus et al., 2015; Sarigil et al., 2019; Yaman and Tekin, 2020; Baskan et al., 2022). The magnetic levitation platform comprises two permanent magnets with the same poles facing each other, a capillary channel containing cells of interest spiked in a paramagnetic medium, and two tilted mirrors for observation via a microscope. Exposed to the magnetic gradient, diamagnetic cells tend to migrate to the lower magnetic field area and levitate at a stable position, where the magnetic force is balanced with the buoyant force, due to the unique densities and diamagnetic properties of objects (Sarigil et al., 2021). With this method, label-free cancer drug analysis (Delikoyun et al., 2021), cardiomyocyte sorting (Puluca et al., 2020), and separation of sperm cells from endothelial cells (Urey et al., 2021) were demonstrated. However, the sorted cells have significantly high levitation heights ($>100$ μm), resulting in a substantial density difference ($>0.05$ g mL$^{-1}$), when compared to the remaining cell populations (Urey et al.; Chin et al.; Delikoyun et al.).

This study demonstrates the sorting of cancer cells from WBCs based on smaller density differences ($\sim 0.01$ g mL$^{-1}$) in a microfluidic chip using the magnetic, gravitational and drag forces (Fig. 1). The microfluidic chip with one inlet, and two outlets was fabricated from polydimethylsiloxane (PDMS) using soft lithography and it was positioned between two opposing magnets. The microseparator in the microfluidic channel was located at the middle of the channel, so that cells were intended to be directed to the top or bottom outlets according to their levitation heights by ensuring equal hydraulic resistance in the top and bottom outlets under a microfluidic flow. Here, cancer cells with lower densities rather than WBCs were directed to the top outlet, while WBCs with higher densities are collected from the bottom outlet. For sorting experiments, optimization of flow rate and paramagnetic agent concentrations was achieved using different densities of microparticles. Then, the label-free sorting performance of the hybrid microfluidic device was tested by using invasive MDA-MB-231 and non-invasive MCF-7 breast cancer cells, as well as U-937 human monocytes. This hybrid μDACS platform allows density-associated cell sorting in a microfluidic channel and is a promising tool for rapid, low-cost, portable, label-free, and effective sorting of rare cancer cells. In addition, collected cells had high viability and these cells could be used for further analysis, including personalized and precision medicine.

## 2. Materials and methods

### 2.1. Materials

Propylene glycol monomethyl ether acetate (PGMEA, Sigma Aldrich, Missouri, USA.), SU-8100 Negative Photoresist (MicroChem, USA), silicon wafers (Nanografi Co. Ltd., Ankara, Turkey), PDMS (Sylgard 184, Dow Corning, USA), and glass slides (Marienfeld, Germany) were acquired for microfabrication of microfluidic chip. Needles (C3 Technology, Turkey) were purchased to punch inlets/outlets. Tygon Microbore Tubing was obtained from Cole Parmer, USA to make fluidic connections to the chip. N52 grade neodymium magnets (Supermagnete, Germany) and microcapillary tubes (Vitrocom, USA) were acquired for the magnetic levitation experiments. Formlabs Form 2 (Formlabs, USA) and Creality CR10S Pro V2 (Creality, China) were used to fabricate 3D printed structures. Polyethylene microspheres with different densities and sizes were purchased from Cospheric LLC, USA. Gadavist® ($Gd^{3+}$) was obtained from Bayern, Germany, and Pluronic F-127 (Sigma Aldrich, USA) was purchased to be used in experiments. 70% ethanol (K50690883 844, Merck, Germany) and isopropanol (VWR Int., Germany) were also acquired. RPMI (Rosewell Park Memorial Institute, Gibco Thermo Fischer Scientific) and DMEM (Dulbecco's modified Eagle's high glucose, Gibco Thermo Fischer Scientific), fetal bovine serum (FBS) (Gibco, Thermo Fischer Scientific), phosphate-buffered saline (PBS) (Gibco, Thermo Fischer Scientific), penicillin−streptomycin (Euroclone, Italy) were purchased for cell studies. Cell culture plates (6–10 cm$^2$) were bought from Euroclone, Italy.

### 2.2. μDACS platform

The platform consists of (i) two N52-grade neodymium magnets (i.e., bottom and top magnets) having 50 mm length × 2 mm width × 5 mm height with a polarization through their height, (ii) a PDMS microfluidic chip where microspheres/cells were levitated and sorted in a paramagnetic medium, and (iii) four mirrors placed at 45° to monitor levitated microspheres/cells using a Zeiss Axio Vert A1 inverted fluorescence microscope (ZEISS, Switzerland) (Fig. 1A). These components of the platform were assembled in a 3D-printed structure fabricated using a 3D printer (Creality CR-10s Pro V2). The chip was fabricated as given in supplementary information (Figs. S1 and S2) and

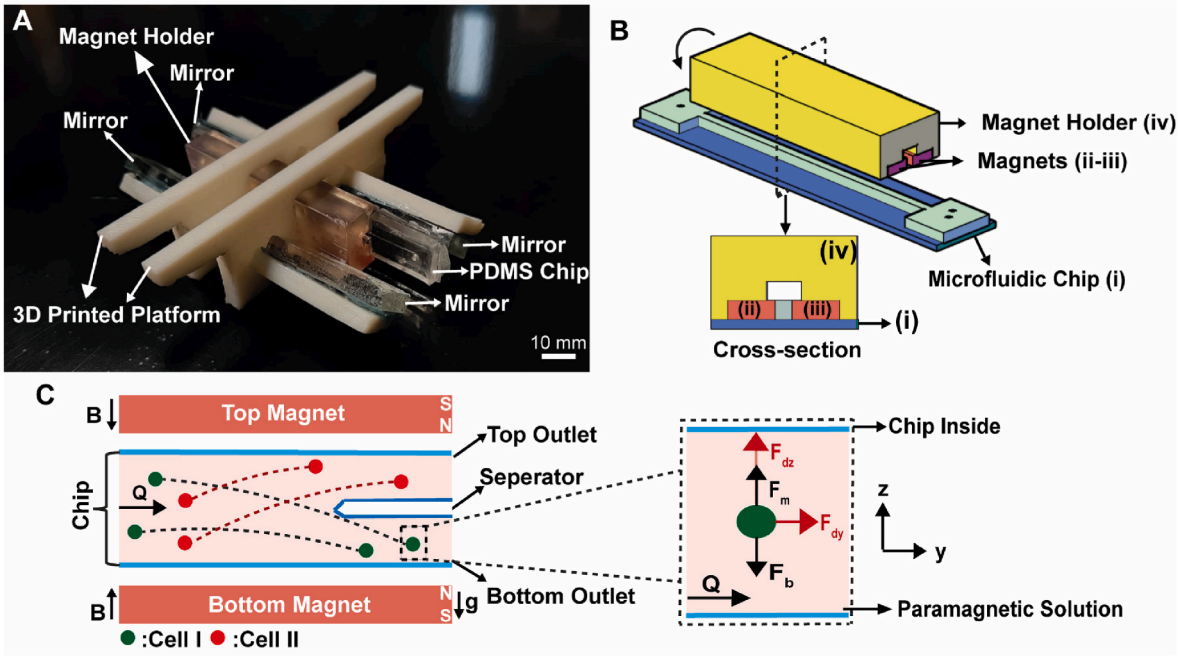


**Fig. 1.** μDACS platform. A. PDMS microfluidic channel placed between two permanent neodymium magnets, whose same poles are facing each other, on the magnet holder. Mirrors are used to image samples along the side of the channel. B. Magnets-chip assembly. The chip (i) was placed between top (ii) and bottom (iii) magnets in the magnet holder (iv) before introducing it in the platform. C. Working principle of the platform. Cells were dragged ($F_{dy}$) with a flow (Q) while they were levitated to a stable height based on their densities under magnetic ($F_m$) and buoyant ($F_b$) forces where drag forces in the z-direction ($F_{dz}$) become zero. Hence, cells with lower densities (Cell II) were collected from the top outlet while other cells (Cell I) were directed to the bottom outlet. g is the gravitational acceleration, and B is the magnetic induction.

it was attached to the magnet holder, which was fabricated using a desktop stereolithographic 3D printer (Form 2) from a transparent resist, between two magnets separated ~1.8 mm from each other (Fig. 1B) and placed in the platform. Then, the chip was connected to the syringe pumps via tubings from chip outlets (Fig. S3). The cell solution was placed on a microtube on a vortex mixer and connected to outlet of the chip with tubing. By using withdrawal mode of syringe pumps, cells were introduced in the channel. During this operation, the pumps were operated to have same flow rates at the outlets, and gentle vortexing was applied to cell solution to eliminate sedimentation.

### 2.3. Density measurements

Polyethylene microspheres with different standard densities, 1.00 g $mL^{-1}$ (with size of 10–20 μm), 1.02 g $mL^{-1}$ (with size of 10–20 μm), 1.05 g $mL^{-1}$ (with size of 45–53 μm), 1.07 g $mL^{-1}$ (with size of 10–20 μm), and 1.09 g $mL^{-1}$ (with size of 20–27 μm) were levitated in the medium containing 30 mM $Gd^{3+}$. The density of these microspheres can vary ±0.005 g $mL^{-1}$ accordingly to the manufacturer. The microsphere solution was loaded into a glass microcapillary tube (50 mm length × 1 mm width × 1 mm height) with a wall thickness of 0.2 mm, and the microcapillary tube was placed between two opposing magnets in the levitation platform. Levitated microspheres were visualized at 5 × under the inverted fluorescence microscope after microspheres reached the equilibrium position within ~10 min in the platform. The levitation heights of the microspheres (distance from the upper border of the bottom magnet) were determined using the ImageJ software. According to the levitation heights of the microspheres, density (g $mL^{-1}$) versus levitation height (μm) graphs were plotted to obtain the calibration curve for density measurements (Fig. S4). Thus, densities can be determined by looking at the levitation heights of the cells/microspheres inside the capillary tube.

### 2.4. Sorting of microspheres

The sorting of microspheres has been carried out in the microfluidic chip. For this purpose, microspheres with different densities measured in the same platform as 1.016 ± 0.02 g $mL^{-1}$ (i.e., 1.02 g $mL^{-1}$ standard density microspheres) and 1.089 ± 0.016 g $mL^{-1}$ (i.e., 1.09 g $mL^{-1}$ standard density microspheres) were prepared in PBS containing 1% Pluronic and 15–60 mM $Gd^{3+}$. Then, the microsphere solution was introduced in the microfluidic channel at different flow rates of 5–20 μL $min^{-1}$. Pluronic, a nonionic surfactant, was used to eliminate the sticking of microspheres on the channel surface that could improve the sorting performance (Khattak et al., 2005). Pluronic concentration was not expected to alter cell viability (Tekin et al., 2013). The sorting efficiencies of microspheres from the top outlet were calculated.

### 2.5. Sorting of cells

For cell sorting experiments, we used MDA-MB-231, MCF-7 and U-937 cell lines having densities of 1.079 ± 0.0077 g $mL^{-1}$, 1.07 ± 0.0139 g $mL^{-1}$, and 1.09 ± 0.0072 g $mL^{-1}$, and diameters of 16.3 ± 1.88 μm, 15.27 ± 1.9 μm and 15.42 ± 2.8 μm respectively. Breast cancer cell lines (either MDA-MB-231 or MCF-7) were mixed with WBCs (U-937) to model cancer patient blood samples. The cells were prepared in 1% Pluronic-FBS containing 5–30 mM of $Gd^{3+}$ at final concentrations of 1 × $10^2$ –1 × $10^3$ breast cancer cells $mL^{-1}$ and 1 × $10^6$ WBCs $mL^{-1}$, respectively. $Gd^{3+}$ is a biocompatible solution and it does not show an adverse effect on cells up to moderate concentration levels (≤200 mM) (Anil-Inevi et al., 2018). For the experiments, 1 mL cell solution was introduced inside the microfluidic channel at a flow rate of 1 mL $h^{-1}$. Then, sorted cells were analyzed under an inverted fluorescence microscope to identify the red fluorescent protein (dsRed) labeled breast cancer cells in the presence of WBCs, and the sorting efficiencies from the top outlet were evaluated.

### 2.6. Viability assay

MBA-MB-231 cells, which are not labeled with dsRed, with a concentration of $1 \times 10^3$ cells $mL^{-1}$ were sorted in 15 mM $Gd^{3+}$ and collected from the top outlet. For the viability comparison before sorting, two control groups were used. One of these was $1 \times 10^3$ cells $mL^{-1}$ solution in FBS without $Gd^{3+}$ (Control I). In the other one, the cell solution contained 15 mM $Gd^{3+}$ (Control II). Cell viability assay (calcein-AM/propidium iodide, Sigma-Aldrich) on sorted cells was performed immediately. The stained cells were imaged under an inverted fluorescence microscope.

## 3. Results and discussion

### 3.1. Modeling of hybrid platform

The developed platform mainly consists of a microfluidic chip and two opposing magnets (Fig. 1C). Cells suspended in a paramagnetic medium are introduced into the platform under continuous flow conditions. This enables the separation of cells based on their different levitation heights, which vary according to their densities. The microseparator integrated into the chip effectively directs the cells into different outlets based on their levitation heights. This mechanism facilitates the collection of cells depending on levitation heights in separate outlets, enabling their retrieval and subsequent analysis.

When the magnetic and buoyant forces are balancing each other in the assembled platform (Fig. 1C), cells reach to stable levitation heights (Sarigil et al., 2021). This final stable levitation height depends mainly on the densities of cells and paramagnetic medium concentration, and it does not depend on cell volume, since volume terms in magnetic and buoyant forces cancel each other (Amin et al., 2017). On the other hand, cells with high volumes can reach this stable height profile rapidly compared to cells with low volumes in the presence of drag forces. In the platform, the sorting efficiencies of the cells with different densities and sizes were simulated with different $Gd^{3+}$ concentrations and flow rates (Fig. 2) from simulated trajectories as described in supplementary information with finite element modeling results (Figs. S5–S7). The sortable density value from the top outlet with high efficiency (>80%) is increasing with $Gd^{3+}$ concentration at 15 μL $min^{-1}$ flow rate (Fig. 2A). The sorting efficiency from the top outlet can be improved by increasing $Gd^{3+}$ concentration, but the purity of sorted cells becomes very low during that process. The size of the cells also affects the sorting efficiencies since the velocities induced on cells due to magnetic and buoyant forces are proportional to cell sizes (Norouzi et al., 2017). Although small cells given at a fixed flow rate may not reach a stable levitation height at the end of the channel, large cells (≥15 μm) in the order of WBCs and cancer cells may rapidly reach a stable levitation height under a flow. Hence, the sorting efficiency can be size-dependent at specific density ranges. Moreover, the flow rate can also alter the cell sorting efficiencies (Fig. 2B). By employing low flow rates (≤5 μL $min^{-1}$), it becomes possible to achieve high-efficiency and high-purity sorting between cell densities of ≤1.08 g $mL^{-1}$ and ≥1.09 g $mL^{-1}$, using a concentration of 30 mM $Gd^{3+}$. Notably, this range aligns with the densities of both cancer cells and WBCs. Conversely, raising the flow rate can increase the sorting throughput. While this may reduce sorting efficiency, it can enhance the purity of the sorted cells for lower $Gd^{3+}$ concentrations (≤15 mM) (Fig. 2A). Furthermore, the position of the microseparator also impacts both sorting efficiency and purity of cells within different density ranges (Fig. S8). To ensure consistent sorting performance across various chips, maintaining a consistent separator position becomes very crucial.

### 3.2. Sorting efficiency of microspheres

We tested the sorting performance of our platform with two different microspheres having 1.016 ± 0.02 g $mL^{-1}$ (green microspheres) and 1.089 ± 0.016 g $mL^{-1}$ (red microspheres) measured densities, and 18.3 ± 3.3 μm (green microspheres) and 22.87 ± 3.65 μm (red microspheres) diameters, respectively (Fig. 3A and B). In the microfluidic channel, most of the low- and high-density microspheres (i.e., green and red microspheres) were collected above and below the microseparator, respectively, using 30 mM $Gd^{3+}$. Hence, it was expected that low-density microspheres would be sorted from the top outlet with high efficiency under a flow. In accordance, 86–90% sorting efficiency was achieved for low-density microspheres up to 15 μL $min^{-1}$ flow rate (Fig. 3C). On the other hand, the sorting efficiency of high-density microspheres was only 4–10%. Although simulations demonstrated 100% sorting efficiency for low-density microspheres and 43.9% sorting efficiency for high-density microspheres (Fig. 2A), experimental conditions resulted in a small fraction of low-density microspheres being collected from the bottom

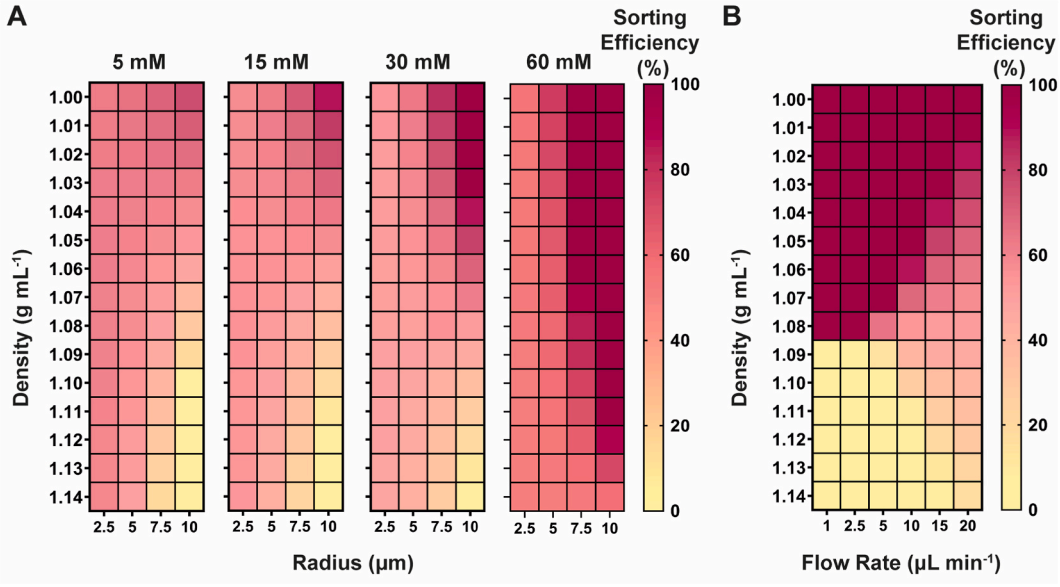


**Fig. 2.** Simulated sorting efficiencies of cells from the top outlet of the microfluidic chip. A. Sorting efficiencies for different cell densities and radii under 15 μL $min^{-1}$ flow rate using 5 mM, 15 mM, 30 mM and 60 mM $Gd^{3+}$. B. Sorting efficiencies for different cell densities with 10 μm radius using different flow rates and 30 mM $Gd^{3+}$.

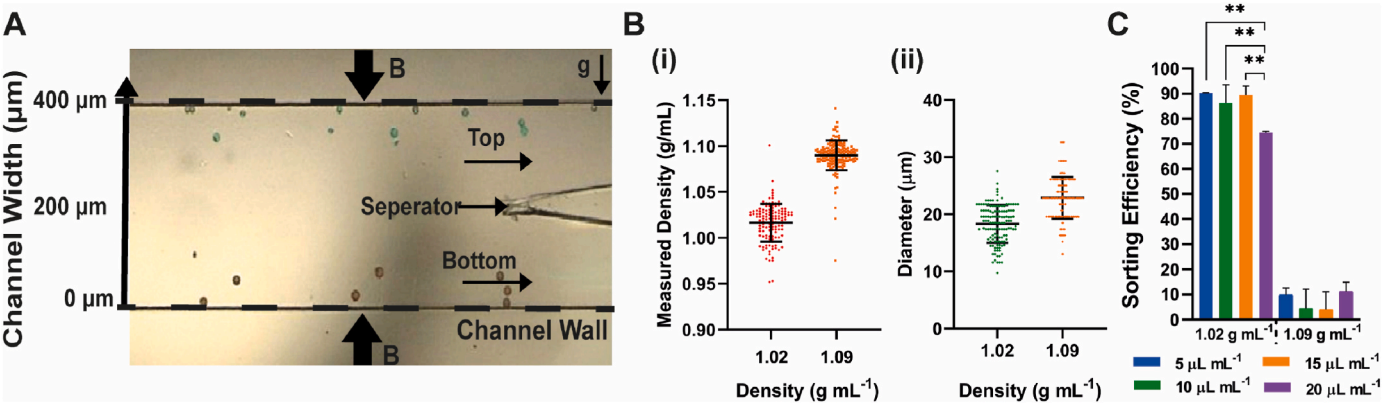


**Fig. 3.** Sorting of microspheres A. Micrograph of levitated different density microspheres in the microfluidic channel. Microspheres with 1.016 g $mL^{-1}$ (green fluorescence) and 1.089 g $mL^{-1}$ (red fluorescence) mean densities were levitated at 30 mM $Gd^{3+}$ concentration. *B* and *g* represent magnetic induction and gravitational acceleration. B. Measured (i) densities and (ii) diameters of microspheres. C. Sorting efficiency of microspheres collected from the top outlet of the microfluidic chip under different fluidic flows using 30 mM $Gd^{3+}$. A one-way ANOVA with Tukey multiple comparison test was used for statistical analysis. Statistical significance (**) indicates $p < 0.01$. (For interpretation of the references to colour in this figure legend, the reader is referred to the Web version of this article.)

outlet and high-density microspheres being collected from the top outlet. This discrepancy can be attributed to the possibility that microspheres with higher densities have larger diameters than those simulated (Fig. 3B), resulting in increased magnetic force-induced velocity, and enabling the microspheres to reach a final stable levitation height during their flow in the microfluidic channel, thereby improving sorting purity even at high flow rates. For instance, as the size of the microspheres increases, they reach a stable final levitation height earlier within the microfluidic channel as shown in simulations (Fig. S7 and Fig. S9). Interestingly, while some microspheres with a density of 1.08 g $mL^{-1}$ and a radius of 10 μm are collected from the top outlet, all microspheres with the same density but a radius of ≥20 μm are collected from the bottom outlet. Additionally, the wide density range of the microspheres (Fig. 3B) can impact the overall sorting efficiency. At high flow rates (20 μL $min^{-1}$), sorting efficiency was statistically reduced for low-density microspheres, since microspheres may not reach stable levitation heights. Moreover, reducing $Gd^{3+}$ concentration to 15 mM decreased the sorting efficiency of low-density microspheres while the sorting efficiency of high-density microspheres remained similar (Fig. S10). On the other hand, increasing $Gd^{3+}$ concentration to 60 mM improved the sorting efficiency of high-density microspheres that could reduce the purity of sorted low-density microsphere (Fig. S10). Hence, 30 mM $Gd^{3+}$ showed the best sorting performance for low- and high-density microspheres at flow rates of ≤15 μL $min^{-1}$. The sorting efficiency data were also presented in Table S1.

### 3.3. Sorting efficiency of cancer cells

Cancer patient blood samples containing CTCs were simulated by mixing breast cancer cells (either MDA-MB-231 or MCF-7) with WBCs (U-937) at specific cell concentrations in FBS. Since cell viability is an important factor that can alter the cell levitation height (Anil-Inevi et al., 2018), we ensured the cell viability before the sorting experiments (Fig. S11). The breast cancer cells have lower densities than WBCs (Norouzi et al., 2017; Fehm et al., 2018) so that they were expected to levitate to a higher position (Fig. 4A and B) and can be collected from the top outlet. However, densities of breast cancer cells and WBCs overlap (Fig. 4A and B). The flow rate of 1 mL $h^{-1}$ (~16.66 μL $min^{-1}$) was selected for sorting cancer cells, as it demonstrated favorable separation efficiency for low-density microspheres (Fig. 3C and Fig. S10).

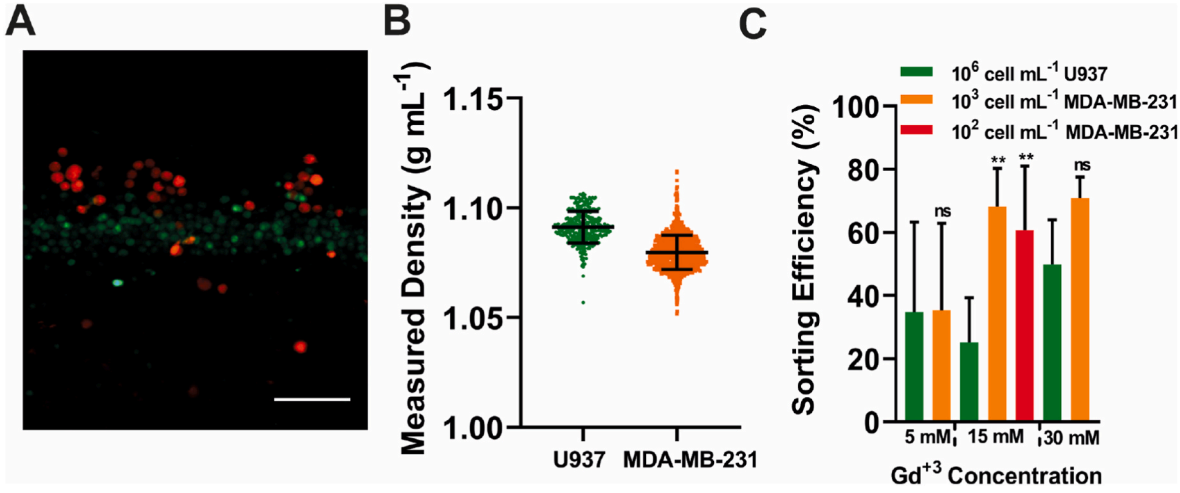


**Fig. 4.** Cell sorting experiments. A. Micrographs of MDA-MB-231 (red) and U-937 (green) cells in the levitation platform. The scale bar is 200 μm. B. Measured cell densities. C. Sorting efficiencies of MDA-MB-231 cells and U-937 cells at different $Gd^{3+}$ concentrations. In the experiments, MDA-MB-231 cells were mixed with U-937 cells in different concentrations. The statistical analysis was made using *t*-test by comparing the sorting results of MDA-MB-231 cells with the results of U-937 cells. ns and ** indicate $p > 0.05$ and $p < 0.01$, respectively. (For interpretation of the references to colour in this figure legend, the reader is referred to the Web version of this article.)

Moreover, this flow rate falls within the commonly utilized range for CTC separation (Ferreira et al.). Hence, sorting conditions should be adjusted precisely to sort breast cancer cells with high efficiency and purity. Low sorting efficiencies (<40%) were observed for MDA-MB-231 with a cell concentration of $1 \times 10^3$ cells $mL^{-1}$ and U-937 cells with a cell concentration of $1 \times 10^6$ cells $mL^{-1}$ using a flow rate of 1 mL $h^{-1}$ and low (5 mM) $Gd^{3+}$concentration (Fig. 4C). By increasing $Gd^{3+}$concentration to 15 mM, the sorting efficiency was increased to 68.3% for MDA-MB-231, while the sorting efficiency for U-937 cells showed a similar profile as in 5 mM $Gd^{3+}$. On the other hand, increasing $Gd^{3+}$ concentration to 30 mM did not alter the MDA-MB-231 sorting efficiency much, but increased U-937 sorting efficiency to 49.9%. Increasing the $Gd^{3+}$ concentration increased the levitation heights of the cells so that maximum collectible cell densities from the top outlet of the chip would be increased, as shown in simulations (Fig. 2). Hence, the purity of sorted breast cancer cells would be decreased with increased $Gd^{3+}$ concentration. Moreover, decreasing the breast cancer cell concentration to $1 \times 10^2$ cells $mL^{-1}$ does not change the sorting efficiency of cells spiked in 15 mM $Gd^{3+}$. On the other hand, it is important to note that the sorting efficiency of cells at various $Gd^{3+}$ concentrations may exhibit a higher standard deviation compared to experiments conducted with microspheres (Tables S1 and S2). This variability can be attributed to potential issues in chip fabrication, which may lead to alterations in the separator's position relative to the magnets. Such alterations can impact the sorting performance of cells with small density differences. Furthermore, the broad density distribution of cells, resulting from cellular heterogeneity and biological conditions such as the presence of live/dead cell populations (Delikoyun et al., 2021) within cell culture batches, can further contribute to variations in sorting performance. The sorting strategy was also evaluated with MCF-7 breast cancer cell line using a flow rate of 1 mL $h^{-1}$ and 15 mM $Gd^{3+}$. The sorting efficiency of MCF-7 cells was also higher than the sorting efficiency of WBCs (Fig. S12). On the other hand, the sorting efficiency of MCF-7 cells was lower than MDA-MB-231 cell sorting efficiency under the same experimental condition. This can be a reason for the wide-density distribution of MCF-7 cells (Fig. S13). The sorting efficiency data of cells were also presented in Table S2.

Furthermore, the viability of sorted cells was studied. Sorted MDA-MB-231 cells showed similar high viability compared to control groups as before sorting experiments (Fig. 5). Hence, the sorting did not alter the cells' viability so that sorted cells could be used for further cell culture analysis.

Several label-free magnetic-based particle/cell sorting methods were already reported in the literature (Table S3). In these methods, size or magnetic property or density differences of particles/cells were used for label-free sorting. For size-based separation, large size differences (i.e., 0.6 to 5-fold difference) are necessary to effectively separate particles/cells (Peyman et al., 2009; Tarn et al., 2009; Vojtíšek et al., 2012; Kawano and Watarai, 2012; Shen et al., 2012). Hence, they cannot be applied to separate CTCs from WBCs, which can have small size differences (Zhou et al., 2019). To apply adequate magnetic forces on particles, superconducting magnets, and ferromagnetic patterns, which can increase the cost of analysis, can also be applied in these methods (Tarn et al., 2009; Vojtíšek et al., 2012; Kawano and Watarai, 2012). The difference in magnetic properties was also used to separate oxygenated and deoxygenated red blood cells (RBCs) with 1.7-fold magnetic susceptibility difference (Seo et al., 2010). Magnetic-based methods were also applied to separate cells using density differences (Urey et al., 2021; Chin et al., 2020; Liang et al., 2022). However, these methods were only used to separate cells with comparably high-density differences (i.e., >0.07-fold difference) (Urey et al., 2021; Chin et al., 2020; Liang et al., 2022), such as sperm cells (having density of 1.165 g $mL^{-1}$) (Stuhtmann et al., 2012) from endothelial cells (1.082 g $mL^{-1}$) (Moser et al., 1992) and live MDA-MB-231 cells (1.16 g $mL^{-1}$) (Delikoyun et al., 2021) from dead MDA-MB-231 cells (1.06 g $mL^{-1}$) (Delikoyun et al., 2021). On the other hand, very small single-cell density differences need to be handled

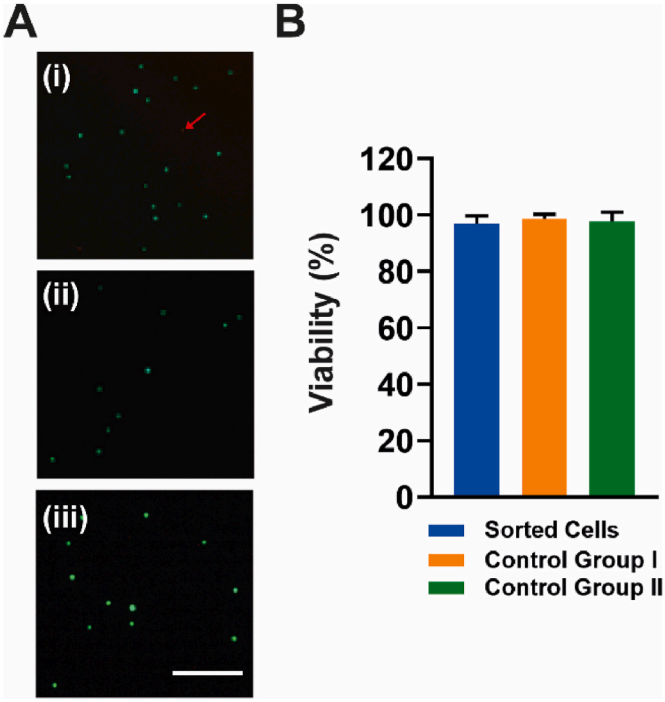


**Fig. 5.** Viability of MDA-MB-231 cells in different conditions. A. Fluorescent images of (i) MDA-MB-231 cells collected from the top outlet, (ii) control cell group I, which contains MDA-MB-231 cells before sorting, and (iii) control cell group II, which contains MDA-MB-231 cells treated with $Gd^{3+}$. Cells were stained with Calcein/PI. The scale bar is 200 μm. B. Cell viability (%) of each group. Data are plotted as the mean of replicates with error bars (±SD) and statistically analyzed using a one-way ANOVA with Tukey multiple comparison test. Non-significant differences were observed between groups.

in magnetic-based technology in order to separate cancer cells from WBCs (Durmus et al., 2015). Furthermore, the previously presented methods were not practiced in separating rare cells, which are <0.1% of the total cell population (Talasaz et al., 2009). However, in our method, small density differences (i.e., >0.01-fold difference) can be used to separate CTCs (0.01–0.1% of the total population) from background population rapidly (1 mL $h^{-1}$) without using any labels. The performance of magnetic levitation-based sorting was significantly improved by employing a microfluidic chip equipped with a microseparator under a continuous flow. In contrast, existing literature utilizes simple channels such as commercially available capillaries (Durmus et al., 2015) or channels fabricated using double-sided adhesive materials (Baday et al., 2022) that do not provide the required level of precision in the channel architecture for sorting. Hence, our methods could show superior performance compared to existing magnetic-based techniques. Moreover, hybrid sorting methods, combining both active and passive sorting techniques, have also been reported (Table S4). These methods typically rely on sorting particles or cells based on differences in size. However, some hybrid approaches require multi-stage separation processes and rely on complex channel geometries (Altay et al., 2022; Kim et al., 2022). Furthermore, relying solely on the size as a sorting parameter for CTCs may not yield high sorting efficiencies, as CTC sizes often overlap with those of blood cells. In hybrid methods, the utilization of electrical or dielectric properties, as well as labeling with surface biomarkers, can enhance the purification of sorting (Islam and Chen, 2023; Varmazyari et al., 2022; Zhang et al., 2018a,b; Zhou et al., 2019). In contrast, our platform enables rapid and label-free sorting of particles and cells with minimal density differences using a simple channel geometry.

Our hybrid microfluidic platform uses density as a biophysical marker to sort cancer cells from WBCs in the microfluidic channel. This sorting strategy using magnetic, gravitational, and drag forces is

independent of cell surface labeling steps. Even when the mean cell densities are very close to each other (~0.011 g $mL^{-1}$ difference), we achieved ~70% sorting efficiency of cancer cells whereas sorting efficiency of WBCs is ~31% from the top outlets under a flow rate of 1 mL $h^{-1}$. To enhance the density difference between cells and improve the sorting efficiency and purity of cancer cells, a promising strategy involves the negative labeling of WBCs using high-density microparticles. This approach can effectively amplify the contrast in density between the target cancer cells and the background cell populations, leading to improved sorting performance and increased purity. In parallel, flow-invasive magnetic elements could be integrated into the microfluidic channel to enhance magnetic-induced velocities on cells and enable sorting at high flow rates (Smistrup et al., 2006; Cornaglia et al., 2014). However, the incorporation of such elements would involve microfabrication steps, which could potentially increase the overall cost of analysis. Since the current cost of our platform is only ~13$ (Table S5), parallel processing could also be conducted on multiple devices to increase the throughput with a tolerable increase in the analysis cost. Moreover, the presented method could be cascaded with different label-free or label-based sorting technologies to improve sorting performance. Sortable density intervals of separated cells can be controlled by changing magnetic forces applied on the cells with $Gd^{3+}$ concentration. Therefore, the platform could be further tuned for sorting different cells.

## 4. Conclusions

There are many difficulties in CTC sorting studies due to the low abundance of CTCs in blood, heterogeneity of surface biomarkers in CTC populations, and reduced cell viability with sorting. Those challenges revealed the importance of investigation and the urgent need for a detection system for rare cancer cells. In this study, it has been shown that our principle used as a new magnetic levitation-based cytometry technique can reduce some of these limitations by using density as a physical biomarker to sort cancer cells. In this way, cancer cells with a minute density difference than WBCs have been sorted efficiently (~70%) for the first time in a hybrid platform using a microseparator integrated microfluidic chip without labels. On the other hand, further efforts are required to enhance the sorting efficiency and purity of cancer cells through the sequential application of various sorting techniques or negative labeling. The developed hybrid microfluidic platform can be used for rapid, low-cost, and label-free separation of cells and microspheres based on their densities. Since the sorted cells maintain their viability, they might further be collected for downstream analysis that could be used for personalized medicine.

## CRediT authorship contribution statement

**Seren Kecili:** fabricated the platform, the mold, and the microfluidic chip, cultured the cells, performed simulations, analyzed the data, designed and regulated the figures, wrote the manuscript. **Esra Yilmaz:** designed the chip, the platform, and the mold, fabricated the platform, the mold, and the microfluidic chip, calibrated the sorting system with microspheres, cultured the cells, analyzed the data, wrote the manuscript. **Ozge Solmaz Ozcelik:** performed the cell sorting experiments, performed simulations, analyzed the data, wrote the manuscript. **Muge Anil-Inevi:** performed the cell viability tests. **Zehra Elif Gunyuz:** performed cell labeling. **Ozden Yalcin-Ozuysal:** performed cell labeling, edited the manuscript. **Engin Ozcivici:** conceived and designed the study, edited the manuscript. **H. Cumhur Tekin:** conceived and designed the study, analyzed the data, wrote the manuscript, edited the manuscript.

## Declaration of competing interest

The authors declare the following financial interests/personal relationships which may be considered as potential competing interests: Authors (H.C.T., E.O., E.Y.) have a patent application (PCT/TR2021/050456) related to the invention presented in this manuscript.

## Data availability

Data will be made available on request.

## Acknowledgements

H.C.T. gratefully acknowledges financial support from The Scientific and Technological Research Council of Türkiye (116M298), Türkiye, Turkish Academy of Science (TUBA-GEBIP 2020), Türkiye, and Science Academy (BAGEP), Türkiye. S.K. acknowledges the support of Turkish Council of Higher Education, Türkiye for 100/2000 CoHE doctoral scholarship. The authors would like to thank Meltem Elitas, Ph.D. from the Department of Mechatronics Engineering, Sabanci University, Türkiye for providing U-937 cell lines and helpful discussions. The authors would like to also thank Research and Application Center for Quantum Technologies (KUANTAM), IZTECH, Türkiye and Lutfi Ozyuzer, Ph.D. from the Department of Physic, IZTECH for providing cleanroom facilities. The authors would like to thank National Nanotechnology Research Center (UNAM), Türkiye for its support for microfabrication. S.K. and O.S.O. would like to thank Oyku Doyran from the Department of Bioengineering, IZTECH for her helpful support during the experiments.

## Appendix A. Supplementary data

Supplementary data to this article can be found online at https://doi.org/10.1016/j.biosx.2023.100392.

## References

Aghilinejad, A., Aghaamoo, M., Chen, X., 2019. On the transport of particles/cells in high-throughput deterministic lateral displacement devices: implications for circulating tumor cell separation. Biomicrofluidics 13 (3).

Allard, W.J., Matera, J., Miller, M.C., Repollet, M., Connelly, M.C., Rao, C., et al., 2004. Tumor cells circulate in the peripheral blood of all major carcinomas but not in healthy subjects or patients with nonmalignant diseases. Clin. Cancer Res. 10 (20), 6897–6904.

Altay, R., Yapici, M.K., Koşar, A., 2022. A hybrid spiral microfluidic platform coupled with surface acoustic waves for circulating tumor cell sorting and separation: a numerical study. Biosensors 12 (3), 171.

Amin, R., Knowlton, S., Dupont, J., Bergholz, J.S., Joshi, A., Hart, A., et al., 2017. 3D-printed smartphone-based device for label-free cell separation. Journal of 3D printing in Medicine 1 (3), 155–164.

Anil-Inevi, M., Yaman, S., Yildiz, A.A., Mese, G., Yalcin-Ozuysal, O., Tekin, H.C., Ozcivici, E., 2018. Biofabrication of in situ self assembled 3D cell cultures in a weightlessness environment generated using magnetic levitation. Sci. Rep. 8 (1), 7239.

Baday, M., Durmus, N.G., Calamak, S., Demirci, U., Davis, R.W., Steinmetz, L., et al., 2022. U.S. Patent No. 11,338,290. U.S. Patent and Trademark Office, Washington, DC.

Bankó, P., Lee, S.Y., Nagygyörgy, V., Zrínyi, M., Chae, C.H., Cho, D.H., Telekes, A., 2019. Technologies for circulating tumor cell separation from whole blood. J. Hematol. Oncol. 12 (1), 1–20.

Baskan, O., Sarigil, O., Mese, G., Ozcivici, E., 2022. Frequency-specific sensitivity of 3T3-L1 preadipocytes to low-intensity vibratory stimulus during adipogenesis. Anim. Cell Dev. Biol. 58 (6), 452–461.

Bussonnière, A., Miron, Y., Baudoin, M., Matar, O.B., Grandbois, M., Charette, P., Renaudin, A., 2014. Cell detachment and label-free cell sorting using modulated surface acoustic waves (SAWs) in droplet-based microfluidics. Lab Chip 14 (18), 3556–3563.

Campton, D.E., Ramirez, A.B., Nordberg, J.J., Drovetto, N., Clein, A.C., Varshavskaya, P., et al., 2015. High-recovery visual identification and single-cell retrieval of circulating tumor cells for genomic analysis using a dual-technology platform integrated with automated immunofluorescence staining. BMC Cancer 15, 1–13.

Chen, Y., Li, P., Huang, P.H., Xie, Y., Mai, J.D., Wang, L., et al., 2014. Rare cell isolation and analysis in microfluidics. Lab Chip 14 (4), 626–645.

Chin, E.K., Grant, C.A., Ogut, M.G., Cai, B., Durmus, N.G., 2020. CelLEVITAS: label-free rapid sorting and enrichment of live cells via magnetic levitation. bioRxiv, 2020-07. https://doi.org/10.1101/2020.07.27.223917.

Cho, H., Kim, J., Song, H., Sohn, K.Y., Jeon, M., Han, K.H., 2018. Microfluidic technologies for circulating tumor cell isolation. Analyst 143 (13), 2936–2970.

Cornaglia, M., Trouillon, R., Tekin, H.C., Lehnert, T., Gijs, M.A., 2014. Magnetic particle-scanning for ultrasensitive immunodetection On-Chip. Anal. Chem. 86 (16), 8213–8223.
Delikoyun, K., Yaman, S., Yilmaz, E., Sarigil, O., Anil-Inevi, M., Telli, K., et al., 2021. HologLev: a hybrid magnetic levitation platform integrated with lensless holographic microscopy for density-based cell analysis. ACS Sens. 6 (6), 2191–2201.
Dharmasiri, U., Witek, M.A., Adams, A.A., Soper, S.A., 2010. Microsystems for the capture of low-abundance cells. Annu. Rev. Anal. Chem. 3, 409–431.
Ding, X., Peng, Z., Lin, S.C.S., Geri, M., Li, S., Li, P., et al., 2014. Cell separation using tilted-angle standing surface acoustic waves. Proc. Natl. Acad. Sci. USA 111 (36), 12992–12997.
Durmus, N.G., Tekin, H.C., Guven, S., Sridhar, K., Arslan Yildiz, A., Calibasi, G., et al., 2015. Magnetic levitation of single cells. Proc. Natl. Acad. Sci. USA 112 (28), E3661–E3668.
Eifler, R.L., Lind, J., Falkenhagen, D., Weber, V., Fischer, M.B., Zeillinger, R., 2011. Enrichment of circulating tumor cells from a large blood volume using leukapheresis and elutriation: proof of concept. Cytometry B Clin. Cytometry 80 (2), 100–111.
Fehm, T.N., Meier-Stiegen, F., Driemel, C., Jäger, B., Reinhardt, F., Naskou, J., et al., 2018. Diagnostic leukapheresis for CTC analysis in breast cancer patients: CTC frequency, clinical experiences and recommendations for standardized reporting. Cytometry 93 (12), 1213–1219.
Ferreira, M.M., Ramani, V.C., Jeffrey, S.S., 2016. Circulating tumor cell technologies. Mol. Oncol. 10 (3), 374–394.
Gascoyne, P.R., Noshari, J., Anderson, T.J., Becker, F.F., 2009. Isolation of rare cells from cell mixtures by dielectrophoresis. Electrophoresis 30 (8), 1388–1398.
Gossett, D.R., Weaver, W.M., Mach, A.J., Hur, S.C., Tse, H.T.K., Lee, W., et al., 2010. Label-free cell separation and sorting in microfluidic systems. Anal. Bioanal. Chem. 397, 3249–3267.
Hyun, K.A., Kwon, K., Han, H., Kim, S.I., Jung, H.I., 2013. Microfluidic flow fractionation device for label-free isolation of circulating tumor cells (CTCs) from breast cancer patients. Biosens. Bioelectron. 40 (1), 206–212.
Islam, M.S., Chen, X., 2023. Continuous CTC separation through a DEP-based contraction–expansion inertial microfluidic channel. Biotechnol. Prog., e3341
Kawano, M., Watarai, H., 2012. Two-dimensional flow magnetophoresis of microparticles. Anal. Bioanal. Chem. 403, 2645–2653.
Khattak, S.F., Bhatia, S.R., Roberts, S.C., 2005. Pluronic F127 as a cell encapsulation material: utilization of membrane-stabilizing agents. Tissue Eng. 11 (5–6), 974–983.
Kim, S.I., Jung, H.I., 2010. Circulating tumor cells: detection methods and potential clinical application in breast cancer. Journal of Breast Cancer 13 (2), 125–131.
Kim, U., Oh, B., Ahn, J., Lee, S., Cho, Y., 2022. Inertia–acoustophoresis hybrid microfluidic device for rapid and efficient cell separation. Sensors 22 (13), 4709.
Königsberg, R., Obermayr, E., Bises, G., Pfeiler, G., Gneist, M., Wrba, F., et al., 2011. Detection of EpCAM positive and negative circulating tumor cells in metastatic breast cancer patients. Acta Oncol. 50 (5), 700–710.
Lee, A., Park, J., Lim, M., Sunkara, V., Kim, S.Y., Kim, G.H., et al., 2014. All-in-one centrifugal microfluidic device for size-selective circulating tumor cell isolation with high purity. Anal. Chem. 86 (22), 11349–11356.
Liang, K., Yaman, S., Patel, R.K., Parappilly, M.S., Walker, B.S., Wong, M.H., Durmus, N. G., 2022. Magnetic levitation and sorting of neoplastic circulating cell hybrids. bioRxiv, 2022-11. https://doi.org/10.1101/2022.11.03.515127.
Lozar, T., Jesenko, T., Kloboves Prevodnik, V., Cemazar, M., Hosta, V., Jericevic, A., et al., 2020. Preclinical and clinical evaluation of magnetic-activated cell separation technology for CTC isolation in breast cancer. Front. Oncol. 10, 554554.
Morgan, T.M., Lange, P.H., Vessella, R.L., 2007. Detection and characterization of circulating and disseminated prostate cancer cells. Frontiers in Bioscience-Landmark 12 (8), 3000–3009.
Moser, R., Fehr, J., Olgiati, L., Bruijnzeel, P.L., 1992. Migration of Primed Human Eosinophils across Cytokine-Activated Endothelial Cell Monolayers.
Nagrath, S., Sequist, L.V., Maheswaran, S., Bell, D.W., Irimia, D., Ulkus, L., et al., 2007. Isolation of rare circulating tumour cells in cancer patients by microchip technology. Nature 450 (7173), 1235–1239.
Norouzi, N., Bhakta, H.C., Grover, W.H., 2017. Sorting cells by their density. PLoS One 12 (7), e0180520.
Peyman, S.A., Kwan, E.Y., Margarson, O., Iles, A., Pamme, N., 2009. Diamagnetic repulsion—a versatile tool for label-free particle handling in microfluidic devices. J. Chromatogr. A 1216 (52), 9055–9062.
Puluca, N., Durmus, N.G., Lee, S., Belbachir, N., Galdos, F.X., Ogut, M.G., et al., 2020. Levitating cells to sort the fit and the fat. Advanced biosystems 4 (6), 1900300.
Renier, C., Pao, E., Che, J., Liu, H.E., Lemaire, C.A., Matsumoto, M., et al., 2017. Label-free isolation of prostate circulating tumor cells using Vortex microfluidic technology. npj Precis. Oncol. 1 (1), 15.
Sarigil, O., Anil-Inevi, M., Firatligil-Yildirir, B., Unal, Y.C., Yalcin-Ozuysal, O., Mese, G., et al., 2021. Scaffold-free biofabrication of adipocyte structures with magnetic levitation. Biotechnol. Bioeng. 118 (3), 1127–1140.
Sarigil, O., Anil-Inevi, M., Yilmaz, E., Mese, G., Tekin, H.C., Ozcivici, E., 2019. Label-free density-based detection of adipocytes of bone marrow origin using magnetic levitation. Analyst 144 (9), 2942–2953.
Seo, H.K., Kim, Y.H., Kim, H.O., Kim, Y.J., 2010. Hybrid cell sorters for on-chip cell separation by hydrodynamics and magnetophoresis. J. Micromech. Microeng. 20 (9), 095019.
Shamloo, A., Yazdani, A., Saghafifar, F., 2020. Investigation of a two-step device implementing magnetophoresis and dielectrophoresis for separation of circulating tumor cells from blood cells. Eng. Life Sci. 20 (7), 296–304.
Shen, F., Hwang, H., Hahn, Y.K., Park, J.K., 2012. Label-free cell separation using a tunable magnetophoretic repulsion force. Anal. Chem. 84 (7), 3075–3081.
Shields Iv, C.W., Reyes, C.D., López, G.P., 2015. Microfluidic cell sorting: a review of the advances in the separation of cells from debulking to rare cell isolation. Lab Chip 15 (5), 1230–1249.
Sieuwerts, A.M., Kraan, J., Bolt-De Vries, J., Van Der Spoel, P., Elstrodt, F., Smid, M., et al., 2009. Response: re: anti–epithelial cell adhesion molecule antibodies and the detection of circulating normal-like breast tumor cells. JNCI: J. Natl. Cancer Inst. 101 (12), 896–897.
Smistrup, K., Lund-Olesen, T., Hansen, M.F., Tang, P.T., 2006. Microfluidic magnetic separator using an array of soft magnetic elements. J. Appl. Phys. 99 (8).
Stuhtmann, G., Oldenhof, H., Peters, P., Klewitz, J., Martinsson, G., Sieme, H., 2012. Iodixanol density gradient centrifugation for selecting stallion sperm for cold storage and cryopreservation. Anim. Reprod. Sci. 133 (3–4), 184–190.
Talasaz, A.H., Powell, A.A., Huber, D.E., Berbee, J.G., Roh, K.H., Yu, W., et al., 2009. Isolating highly enriched populations of circulating epithelial cells and other rare cells from blood using a magnetic sweeper device. Proc. Natl. Acad. Sci. USA 106 (10), 3970–3975.
Tarn, M.D., Hirota, N., Iles, A., Pamme, N., 2009. On-chip diamagnetic repulsion in continuous flow. Sci. Technol. Adv. Mater. 10, 1. https://doi.org/10.1088/1468-6996/10/1/014611.
Tekin, H.C., Cornaglia, M., Gijs, M.A., 2013. Attomolar protein detection using a magnetic bead surface coverage assay. Lab Chip 13 (6), 1053–1059.
Tomlinson, M.J., Tomlinson, S., Yang, X.B., Kirkham, J., 2013. Cell separation: terminology and practical considerations. J. Tissue Eng. 4, 2041731412472690.
Urey, D.Y., Chan, H.M., Durmus, N.G., 2021. Levitational cell cytometry for forensics. Advanced Biology 5 (3), 2000441.
Varmazyari, V., Ghafoorifard, H., Habibiyan, H., Ebrahimi, M., Ghafouri-Fard, S., 2022. A microfluidic device for label-free separation sensitivity enhancement of circulating tumor cells of various and similar size. J. Mol. Liq. 349, 118192.
Vojtíšek, M., Tarn, M.D., Hirota, N., Pamme, N., 2012. Microfluidic devices in superconducting magnets: on-chip free-flow diamagnetophoresis of polymer particles and bubbles. Microfluid. Nanofluidics 13, 625–635.
Waheed, W., Sharaf, O.Z., Alazzam, A., Abu-Nada, E., 2021. Dielectrophoresis-field flow fractionation for separation of particles: a critical review. J. Chromatogr. A 1637, 461799.
Yaman, S., Tekin, H.C., 2020. Magnetic susceptibility-based protein detection using magnetic levitation. Anal. Chem. 92 (18), 12556–12563.
Yaman, S., Anil-Inevi, M., Ozcivici, E., Tekin, H.C., 2018. Magnetic force-based microfluidic techniques for cellular and tissue bioengineering. Front. Bioeng. Biotechnol. 6, 192.
Yap, T.A., Lorente, D., Omlin, A., Olmos, D., De Bono, J.S., 2014. Circulating tumor cells: a multifunctional biomarker. Clin. Cancer Res. 20 (10), 2553–2568.
Yousuff, C.M., Hamid, N.H.B., Hussain, K.I., Ho, E.T.W., 2016. Numerical modelling and simulation of dielectrophoretic based WBC sorting using sidewall electrodes. In: 2016 6th International Conference on Intelligent and Advanced Systems (ICIAS). IEEE, pp. 1–5.
Zhang, J., Yuan, D., Zhao, Q., Yan, S., Tang, S.Y., Tan, S.H., et al., 2018a. Tunable particle separation in a hybrid dielectrophoresis (DEP)-inertial microfluidic device. Sensor. Actuator. B Chem. 267, 14–25.
Zhang, X., Zhu, Z., Xiang, N., Long, F., Ni, Z., 2018b. Automated microfluidic instrument for label-free and high-throughput cell separation. Anal. Chem. 90 (6), 4212–4220.
Zhao, W., Cheng, R., Miller, J.R., Mao, L., 2016. Label-free microfluidic manipulation of particles and cells in magnetic liquids. Adv. Funct. Mater. 26 (22), 3916–3932.
Zhou, Y., Ma, Z., Ai, Y., 2019. Hybrid microfluidic sorting of rare cells based on high throughput inertial focusing and high accuracy acoustic manipulation. RSC Adv. 9 (53), 31186–31195.
Zhu, Z., Wu, D., Li, S., Han, Y., Xiang, N., Wang, C., Ni, Z., 2021. A polymer-film inertial microfluidic sorter fabricated by jigsaw puzzle method for precise size-based cell separation. Anal. Chim. Acta 1143, 306–314.